Vertically Coupled Quantum-Dot Infrared Photodetectors

Ming-Cheng Lo, Shiang-Yu Wang, Hong-Shi Ling, and Chien-Ping Lee, *Fellow, IEEE*

***Abstract*—Vertically coupled InAs–GaAs quantum-dot infrared photodetectors (QDIPs) were studied in this letter. With vertically coupled quantum dots (QDs), the QDs in the same column share the same electronic states which remove the QD size variation effect in the growth direction and result in a narrow response band and higher peak quantum efficiency. The coupled states increase the capture probability and also facilitate the carrier flow among QD layers. The frequency response of vertically coupled QDIPs is much faster than that of the conventional ones.**

***Index Terms*—Infrared detectors, photodetectors, quantum dots (QDs), quantum effect semiconductor devices.**

IN THE past decade, quantum-dot infrared photodetectors (QDIPs) have been widely investigated with different structures and materials [1]–[5]. The three-dimensional carrier confinement of the quantum-dot (QD) structure provided the possibility to suppress the electron phonon interaction and relax the selection rule of intersubband transitions in the quantum-well structure. QDIPs are thus of great potential to overcome the drawbacks of the commercialized quantum-well infrared photodetectors (QWIPs) and become low-cost and high-temperature operation infrared detectors. With the self-assembled In(Ga)As–GaAs QDs, encouraging results have been demonstrated with operation temperatures over 200 K [3] and even up to room temperature [4]. Furthermore, high-performance 640×512 QDIPs imaging focal plane arrays have also been demonstrated [5].

However, the performance of QDIPs is still limited by the low quantum efficiency which is critical in most applications. The density and uniformity of the QDs are essential for the improvement of the quantum efficiency. Unfortunately, the density and uniformity of QDs are greatly limited by the self-assembled growth process. In addition, poor frequency response of the responsivity in QDIPs was also reported with the roll-off frequency lower than 1 KHz, especially at lower temperatures [6]. Compared with QWIPs, the roll-off frequency is a few orders of magnitude lower for QDIPs. The slow component of photocurrent originated from the recharging process of the electrons into the QDs deteriorates the frequency response [7]. This limits the use of QDIPs in some military and space applications where high-speed detection is demanded.

With thin spacer layers between QD layers, it has been demonstrated that the vertically aligned QDs could be grown and generate shared states among the QD layers [8], [9]. The vertically coupled QD columns allow carriers to diffuse to different QD layers easily. Narrower photoluminescence (PL) spectral width of vertical coupled QDs has been deduced to be from the coupled states which remove the size variation effect in the growth direction [8]. In the past, the infrared absorption of vertically coupled QDs has been reported [10]. In this study, we demonstrated vertically coupled QDIPs (VC-QDIPs) with narrower response spectra and higher response roll-off frequencies.

Two samples were prepared by the Varian Gen-II MBE system on (001) GaAs semi-insulating substrates. Different active regions, sandwiched between two 500-nm silicon-doped contact layers, were used in the two samples. Sample A is a conventional QDIP with 10 periods of 2.6 ML InAs QDs and 50-nm barriers. Each barrier layer consists of a 47-nm GaAs layer and a 3-nm $Al_{0.2}Ga_{0.8}As$ current blocking layer [1]. Sample B is a VC-QDIP with seven periods of InAs QDs and thin 10-nm GaAs spacers. The active region was not doped to keep the low dark current. Due to the growth of the vertical aligned process, the thin AlGaAs blocking layer structure in sample A is not practical in sample B. A 50-nm $Al_{0.27}Ga_{0.73}As$ current blocking layer was inserted on top of the bottom contact layer instead. In order to control the stress in the active region to avoid the generation of dislocations, only seven layers of QDs were grown in sample B. The growth condition for barriers and InAs QDs were kept the same for the two samples.

Sample B was first examined with the high-resolution cross-sectional transmission electron microscopy (TEM) to check the vertical alignment of the QDs. Fig. 1 shows the TEM image of sample B with well-aligned QDs along the growth direction. The QD increases in radius but decreases in height as the layer number increases [8]. The local strain relaxation facilitates the QD's formation directly on the top of the QDs in the previous layer. Such strain relaxation is expected to be reduced with the increase of GaAs capping layer thickness. In sample B, the 10-nm GaAs capping layers were thin enough so that the QDs were aligned in the growth direction. On the other hand, 50-nm capping layers in sample A were too thick for the QDs to be aligned. However, it should be mentioned that from the TEM images, not all of the QD columns in sample B are perfectly aligned for all seven layers. Due to the nonuniform strain distribution, some of the QDs are not well aligned along the QD columns [9].

Manuscript received December 23, 2009; revised March 03, 2010; accepted March 08, 2010. Date of publication March 22, 2010; date of current version May 12, 2010. This work was supported by the National Science Council under Contract NSC98-2112-M-001-020-MY3.

M.-C. Lo and C.-P. Lee are with the Department of Electrical Engineering, National Chiao Tung University, Hsinchu 300, Taiwan.

S.-Y. Wang and H.-S. Ling are with the Institute of Astronomy and Astrophysics, Academia Sinica, Taipei 106, Taiwan (e-mail: sywang@asiaa.sinica.edu.tw).

Color versions of one or more of the figures in this letter are available online at http://ieeexplore.ieee.org.

Digital Object Identifier 10.1109/LPT.2010.2046030

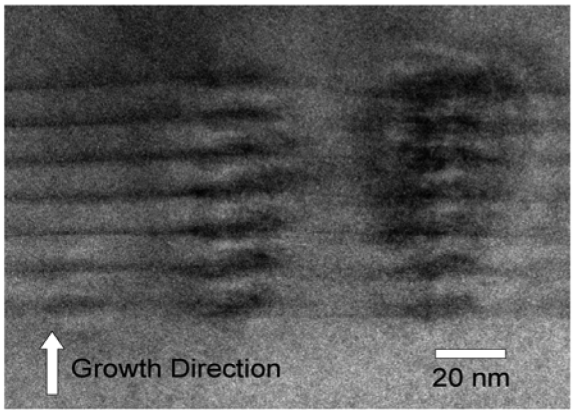

Fig. 1. Cross-section TEM image of sample B.

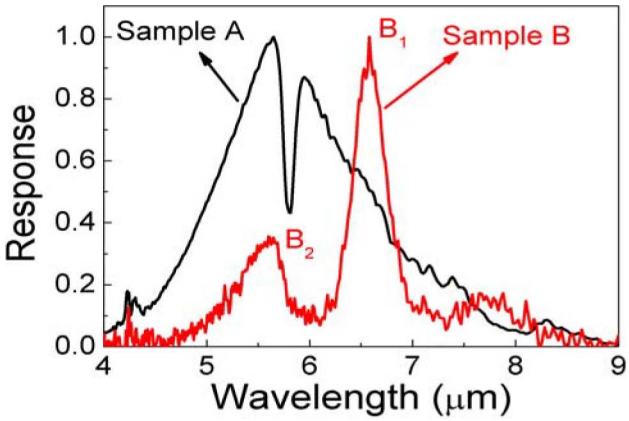

Fig. 2. Normalized photocurrent spectra of samples A and B at 40 K and 0.5 V. The peak responsivity is 0.2 and 0.008 A/W for sample A and sample B, respectively.

The thin GaAs barrier allows the electronic wave functions of QDs in the same column to overlap so that the QDs with different sizes share the same quantum states [8]. The coupling was confirmed by the PL measurement. The 20 K PL spectrum peaks are at 1.17 and 1.01 eV for samples A and B, respectively. The clear redshift of the PL peak in sample B indicates the coupling of the states between the QDs which decreases the lowest ground state energy. In the PL spectrum of sample B, the signal from the uncoupled QDs shown in the TEM result was also detected as a small peak near 1.17 eV.

Individual devices were then produced by standard lithography processes. All measurements were performed with normal incident radiation from the mesa top and the bottom contact was referred as the ground. Fig. 2 shows the normalized photocurrent spectrum of samples A and B at 40 K. The response peak of sample A was about 5.6 μm with the full-width at half-maximum (FWHM) of 1.4 μm. On the other hand, two absorption peaks were observed in sample B. The smaller peak (B2) in sample B is consistent with the response spectrum of sample A. It is associated with the uncoupled QDs. The major signal (B1) was around 6.6 μm and the FWHM was only 0.4 μm($\Delta\lambda/\lambda \sim 0.06$). The FWHM of the photocurrent spectrum of sample B is much narrower than that of sample A. The shared states in the QD layers of sample B provide common states for the intersubband absorption and reduce the

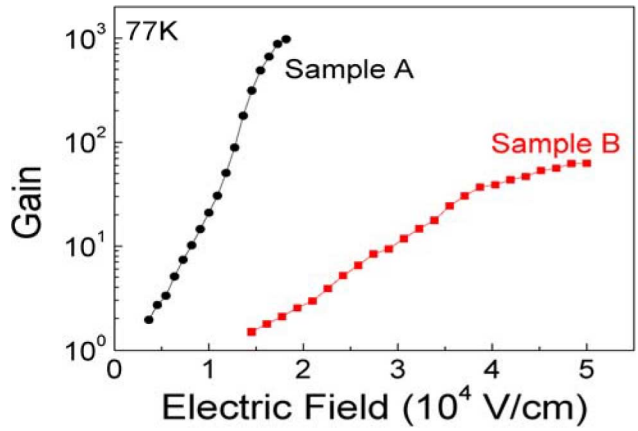

Fig. 3. Noise current gain of samples A and B as a function of the average electric field at 77 K.

FWHM which mainly comes from the size nonuniformity of the QDs in sample A. Although the QDs have three-dimensional confinements, the spectral width of QDIPs is dominated by the size variation in the growth direction which has the smallest physical size. The in-plane size variation still exists in the vertical coupled QDs, but the reduction of the size variation effect in the growth direction effectively reduces the spectral width of the VC-QDIPs. In QWIPs, the devices with mini-bands usually provide wider absorption band than the discrete quantum-well devices due to the broadening of the mini-bands with more than 100 periods of superlattices. In our case, since only seven layers of QDs were used, the coupled states clearly reduced the broadened absorption linewidth caused by the size fluctuation of individual QDs, resulting in narrower absorption spectrum.

Noise measurement was also executed to extract the current gain and the quantum efficiency of the devices. Assuming the generation-recombination noise dominates, the noise current gain of samples A and B at 77 K was shown as a function of average electric field in Fig. 3. A dramatic decrease of the current gain of sample B was clearly observed compared with that of sample A. The gain was a few orders of magnitude lower in sample B under the same electric field. This indicates a major difference in the transport characteristics between the two samples. It is known the noise current gain of QDIPs could be expressed as [11]

$$g = \frac{1 - \frac{P_c}{2}}{FNP_c}$$

where N is number of QD layers, P_c is the capture probability, and F is the filling factor. Since the two samples have a similar filling factor, the capture probability was thus much higher in sample B as the layer number is higher in sample A. The extended electron wavefunction effectively increases the cross section of the QDs and the capture probability of the carriers. Also, it was proposed that the capture probability is connected to the charge inside the QDs [12], [13]. The repulsive charge in the QDs repels the carriers to be captured into the QDs and leads to low capture probability. In sample B, the coupled states facilitate the carrier redistribution between the layers. The chance to generate high repulsive coulomb potential was much lower than that of the conventional QDIPs.

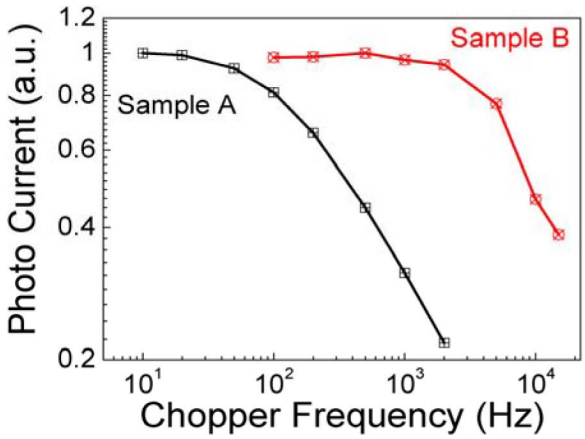

Fig. 4. Normailized frequency response of photocurrent for samples A and B at 40 K and 0.5 V.

The higher capture probability is expected to accelerate the recharging process of the QDs. This was examined by the frequency dependence of the photocurrent. The response photocurrents of the two samples were measured with a standard lock-in technique at different chopper frequencies. The measurement was performed at 0.5 V and 40 K. The dark current density of these two samples at this operation condition was quite close ($\sim 1 \times 10^{-9}$ A/cm^2) to ensure similar carrier flow for the two samples. Fig. 4 shows the normalized frequency response photocurrent of the two samples. The roll-off frequency was only around 500 Hz of sample A but increased to about 8000 Hz of sample B. As expected, the higher capture probability in VC-QDIPs shortens the charging process and greatly increases the roll-off frequency. The roll-off frequency for VC-QDIPs was higher than the measurement limit at 30 KHz at 77 K. It was close to the roll-off frequency of QWIPs.

With the current gain and responsivity measured, the quantum efficiency of the two samples was also calculated. The peak quantum efficiency at 77 K is 0.23% and 0.78% for sample A and sample B, respectively. The narrower bandwidth of the VC-QDIP enhances the quantum efficiency even though only seven layers of QDs were used in sample B. However, the low current gain in sample B counteracts the higher quantum efficiency and leads to lower responsivity in sample B. The responsivity in sample A was about 1 A/W at 0.7 V and 77 K, but it was only 0.1 A/W under the same condition in sample B. At 0.6 V and 60 K, the detectivity for sample A was 1.9×10^{10} cm $\cdot$ Hz$^{0.5}$/W, which was slightly higher than that of sample B (1×10^{10} cm $\cdot$ Hz$^{0.5}$/W). As mentioned, in sample B, some QDs are not well aligned and the layer number is not as high as in sample A. More study on the vertical alignment of the QDs to increase the layer numbers and to avoid the uncoupled QDs will further enhance the quantum efficiency and the performance of the VC-QDIPs.

In summary, VC-QDIPs have been investigated in this study. With the coupled states in QDs, the responsivity spectrum and the roll-off frequency for QDIPs have been improved. The responsivity spectrum showed a fractional spectral width of only 6% which increased the peak quantum efficiency. The enhanced capture probability also increased the roll-off frequency dramatically. The device provided a possible solution to enhance the quantum efficiency and roll-off frequency at the same time. More work to improve the vertical alignment condition of the QDs will further enhance the performance of the VC-QDIPs.

REFERENCES

[1] S. Y. Wang, S. D. Lin, H. W. Wu, and C. P. Lee, "Low dark current quantum-dot infrared photodetectors with an AlGaAs current blocking layer," *Appl. Phys. Lett.*, vol. 78, pp. 1023–1025, 2001.

[2] H. Lim, W. Zhang, S. Tsao, T. Sills, J. Szafraniec, K. Mi, B. Movaghar, and M. Razeghi, "Quantum dot infrared photodetectors: Comparison of experiment and theory," *Phys. Rev. B*, vol. 72, p. 0855332, 2005.

[3] S. Chakrabarti, A. D. Stiff-Roberts, P. Bhattacharya, S. Gunapala, S. Bandara, S. B. Rafol, and S. W. Kennerly, "High-temperature operation of InAs–GaAs quantum-dot infrared photodetectors with large responsivity and detectivity," *IEEE Photon. Technol. Lett.*, vol. 16, no. 5, pp. 1361–1363, May 2004.

[4] P. Bhattacharya, X. H. Su, S. Chakrabarti, G. Ariyawansa, and A. G. U. Perera, "Characteristics of a tunneling quantum-dot infrared photodetector operating at room temperature," *Appl. Phys. Lett.*, vol. 86, p. 191106, 2005.

[5] S. D. Gunapala, S. V. Bandara, C. J. Hill, D. Z. Ting, J. K. Liu, S. B. Rafol, E. R. Blazejewski, J. M. Mumolo, S. A. Keo, S. Krishna, Y. C. Chang, and C. A. Shott, "640 × 512 pixels long-wavelength infrared (LWIR) quantum-dot infrared photodetector (QDIP) imaging focal plane array," *IEEE J. Quantum Electron.*, vol. 43, no. 3, pp. 230–237, Mar. 2007.

[6] D. T. Le, C. P. Morath, H. E. Naoton, D. A. Cardimona, S. Raghavan, P. Rotella, S. A. Stintz, B. Fuchs, and S. Krishan, "High responsivity LWIR dots-in-a-well quantum dot infrared photodetectors," *Infrared Phys. Technol.*, vol. 44, pp. 517–526, 2003.

[7] R. Rehm, H. Schneider, M. Walther, and P. Koidl, "Influence of the recharging process on the dark current noise in quantum-well infrared photodetectors," *Appl. Phys. Lett.*, vol. 80, pp. 862–864, 2002.

[8] G. S. Solomon, J. A. Trezza, A. F. Marshall, and J. S. Harris, "Vertically aligned and electronically coupled growth induced InAs islands in GaAs," *Phys. Rev. Lett.*, vol. 76, pp. 952–955, 1996.

[9] G. S. Solomon, J. A. Trezza, A. F. Marshall, and J. S. Harris, "Structural and photoluminescence properties of growth-induced InAs island columns in GaAs," *J. Vac. Sci. Technol. B*, vol. 14, p. 2208, 1996.

[10] Q. D. Zhuang, J. M. Li, H. X. Li, Y. P. Zeng, L. Pan, Y. H. Chen, M. Y. Kong, and L. Y. Lin, "Intraband absorption in the 8–12 mm band from Si-doped vertically aligned InGaAs/GaAs quantum-dot superlattice," *Appl. Phys. Lett.*, vol. 73, pp. 3706–3708, 1998.

[11] Z. Ye, J. C. Campbell, Z. Chen, E. T. Kim, and A. Madhukar, "Noise and photoconductive gain in InAs quantum-dot infrared photodetectors," *Appl. Phys. Lett.*, vol. 83, pp. 1234–1236, 2003.

[12] V. Ryzhii, I. Khmyrova, M. Ryzhii, and V. Mitin, "Comparison of dark current, responsivity and detectivity in different intersubband infrared photodetectors," *Semicond. Sci. Technol.*, vol. 19, pp. 8–16, 2004.

[13] S. Y. Wang, M. C. Lo, H. Y. Hsiao, H. S. Ling, and C. P. Lee, "Temperature dependent responsivity of quantum dot infrared photodetectors," *Infrared Phys. Technol.*, vol. 50, pp. 166–170, 2007.